ATP-activated Current and Its Interaction with Acetylcholine-activated Current in Rat Sympathetic Neurons

Ken Nakazawa

Department of Neurobiology, Harvard Medical School, Boston, Massachusetts 02115

Ionic current activated by extracellular ATP was characterized using whole-cell voltage clamp of rat sympathetic neurons isolated from superior cervical ganglia. ATP (10–1000 μM) activated an inward current (I_{ATP}) at negative holding potentials in almost all the cells (>97%). The current was reversed near 0 mV in a quasiphysiological external solution, and the concentration dependence could be fitted by a curve with an EC_{50} value of 60 μM and a Hill coefficient of 1.8. The relationship between I_{ATP} and the current activated by ACh (I_{ACh}) was examined. ACh (100 μM) activated an inward current one- to fivefold larger than the current activated by 100 μM ATP. I_{ATP} and I_{ACh} were not additive; the current activated by simultaneous application of ATP and ACh was only as large as the current activated by ACh alone. During current activation by ATP or ACh, the current activated by the other agonist became smaller, suggesting that these agonists reciprocally inhibit their excitatory responses. The reciprocal inhibition appeared to depend on the extent of channel opening because the reduction of the current elicited by each agonist was relieved when the current elicited by the other agonist had been desensitized. Suramin (100 μM), a purinoceptor antagonist, selectively inhibited I_{ATP} whereas two open-channel blockers of nicotinic receptor channels, hexamethonium (10–100 μM) and d-tubocurarine (1–10 μM), inhibited I_{ACh} without affecting I_{ATP}. When 140 mM glucosamine was used as an external cation, only ATP but not ACh activated a considerable inward current at −150 mV. The ATP-induced glucosamine influx was reduced by simultaneous application of ACh. These results suggest that channel activation by ATP and that by ACh are not independent, and these two excitatory neurotransmitters negatively interact with each other at postsynaptic level in rat sympathetic neurons. The interaction between the ATP- and the ACh-induced conductances was hypothetically explained based upon our previous proposal of "channel overlap"; that is, ATP activates a subpopulation of the nicotinic receptor channels.

[Key words: rat, sympathetic neurons, superior cervical ganglia, ATP, ACh, nicotinic receptor, ion channels, voltage clamp]

ATP activates nonselective cation channels in various types of cells including neuronal cells (for reviews, see Bean and Friel, 1990; Bean, 1992; Inoue and Nakazawa, 1992). A physiological role has been suggested for the ATP-activated channels in smooth muscle contraction, as signal transducers in response to purinergic neurotransmission (Burnstock and Kennedy, 1985; Burnstock, 1990a,b) by generating excitatory junctional potentials (e.g., Suzuki, 1985) or by permitting Ca^{2+} influx through the channels themselves (Benham, 1989). Recently, the significance of endogenous ATP and the ATP-activated channels was also demonstrated in neurons. By using suramin, a purinoceptor antagonist (Dunn and Blakely, 1988; Nakazawa et al., 1990a, 1991b), it was shown that ATP acts as a neurotransmitter in guinea pig celiac ganglia (Evans et al., 1992) and a subpopulation of rat medial habenula neurons (Edwards et al., 1992). As the ATP-activated current in these cells has characteristics in common with those reported in other types of cells, contribution of such purinergic transmission to neuronal functions may be more widespread than previously expected.

A concept of the ligand-gated channel superfamily, which includes families of nicotinic receptor channels, glutamate-receptor channels, GABA-receptor channels, and glycine-receptor channels, has been proposed (Betz, 1990; Hille 1992a,b). A subclass of 5-HT receptors (5-HT$_3$ receptor) has recently joined this superfamily (Peters et al., 1992). Each of these families is responsible for postsynaptic signal transduction in fast neurotransmission. ATP-activated channels likely form such a ligand-gated channel family, because (1) ATP activates ion channels in cell-free membrane patches (Benham and Tsien, 1987; Krishtal et al., 1988; Nakazawa et al., 1990c; Neuhaus et al., 1991), and (2) an obvious time lag between ATP application and the beginning of the current was not detectable, and the time constant of the current activation was as small as 10 msec when the ATP application was made by rapid exchange of the solutions around cells (Friel and Bean, 1988; Bean, 1990; Ueno et al., 1992).

Interaction between ATP and nicotinic receptor channels has been suggested. ATP activates ionic channels that have the same conductance as nicotinic receptor channels in chick (Kolb and Wakelam, 1983) and *Xenopus* (Igusa, 1988) skeletal muscle cells. More recently, Lu and Smith (1991) reported that ATP facilitates nicotinic receptor channels by a second messenger–mediated mechanism. The interaction between nicotinic receptor channels and ATP-activated channels was also suggested in rat pheochromocytoma PC12 cells from the observation that the current activated by ATP and that by nicotine were not additive but saturable (Nakazawa et al., 1991a). Such relation between ATP and ACh in channel activation has not been reported in primary neurons.

In the present study, I characterized the ATP-activated current and its interaction with the ACh-activated current in sympathetic neurons enzymatically dispersed from rat superior cervical ganglia. My results suggest that the ATP-activated channels are not independent of the nicotinic receptor channels, and that these two types of ligand-gated channels negatively interact. I hypothesize that this negative interaction arises from the activation by ATP of a subpopulation of the nicotinic receptor channels, which may result in reciprocal modulation of two types of excitatory neurotransmitters at postsynaptic membrane.

Materials and Methods

Cell isolation. Sympathetic neurons were enzymatically dissociated from rat superior cervical ganglia according to Bean (1990) with modification. Long-Evans rats of either sex (14–30 d old) were killed by cervical dislocation, and superior cervical ganglia were immediately dissected. The ganglia were treated first with 24 U/ml papain (Worthington Biochemical, Freehold, NJ), which had been dissolved in 3 ml of Ca^{2+}-free Tyrode's solution [composition (in mM): 150 NaCl, 4 KCl, 2 $MgCl_2$, 10 HEPES; pH was adjusted to 7.4 with NaOH] containing 0.5 mM EDTA and 2 mM D,L-cysteine, and preactivated for 20 min at 35°C. After 20 min of treatment with papain, the solution was replaced with 1.9 mg/ml collagenase (Sigma type I, St. Louis, MO) and 16 mg/ml dispase (Boehringer Mannheim GmbH, Mannheim, Germany) dissolved in 5 ml of Ca^{2+}-free Tyrode's solution for 45 min. During the enzyme treatment, the solution was kept at 35°C and stirred (about 1.5 rpm) with a magnetic stirrer. The solution containing the enzyme-treated ganglia was then centrifuged at 500 rpm for 2 min. The precipitation was resuspended in 5 ml of Leibovitz's L-15 medium (GIBCO, Grand Island, NY), and stored at 4°C. Cells were dispersed by gentle trituration and served for experiments. Experiments were performed within 5 hr after cell harvest.

Membrane current measurement. An experimental chamber containing extracellular solution [composition (in mM): 150 NaCl, 4 KCl, 2 $CaCl_2$, 2 $MgCl_2$, 10 HEPES, 10 glucose; pH 7.4 with NaOH] was mounted on the stage of an inverted microscope (Olympus IMT-2, Tokyo, Japan), and the isolated cells were pipetted into it. Membrane currents were recorded with the whole-cell, voltage-clamp technique (Hamill et al., 1981). Patch pipettes were pulled from 100 μl Boralex micropipettes (Dynalab, Rochester, NY), coated with Sylgard (Dow Corning, Midland, MI), and fire polished. Tip resistance of the patch pipettes ranged from 3 to 4 MΩ when filled with intracellular solution containing 130 mM CsCl, 10 mM HEPES, and 10 mM EGTA (pH 7.4 with CsOH). Currents were recorded with a patch-clamp amplifier (List EPC7, Darmstadt, Germany) through a 3 kHz low-pass filter (−3 dB, 3-pole Bessel) built into the amplifier. Series resistance compensation was employed for the cells where the current activated by ACh or ATP was larger than 500 pA. The compensation was not employed when the current was less than 500 pA because the voltage error in this condition is estimated to be less than 2 mV if tip resistance of 4 MΩ is assumed. Electrical signals were digitized at 0.2–1 kHz using a BASIC-FASTLAB analog/digital interface and software (Indec System, Sunnyvale, CA), and stored for later analyses.

Application of ATP and other compounds was made through an array of parallel microcapillary tubes (Yellen, 1982; Friel and Bean, 1988; Bean, 1990). In this method, two solutions emitted from neighboring tubes were exchanged with a time constant of <100 msec (Friel and Bean, 1988; Bean, 1990), which is much faster than the observed desensitization of the ATP- and the ACh-activated current, which occurred in the order of seconds (e.g., Fig. 5). Thus, the peak of the currents is probably little reduced by the solution exchange. After achievement of a whole-cell recording, the mouth of the tube emitting standard Tyrode's solution was placed in front of the cell for about 1 min, and the array of tubes was then moved so that the cell was exposed to a desired test solution. To avoid desensitization of I_{ATP} or I_{ACh}, exposure to these agonists was brief (1–3 sec) and repeated exposure were separated by 20–40 sec unless otherwise noted. Before examining effects of compounds on I_{ATP} or I_{ACh}, ATP or ACh was applied several times as control until the response became stable. Stable current amplitude was obtained normally up to four times of the application.

For the solution containing glucosamine as a major external cation,
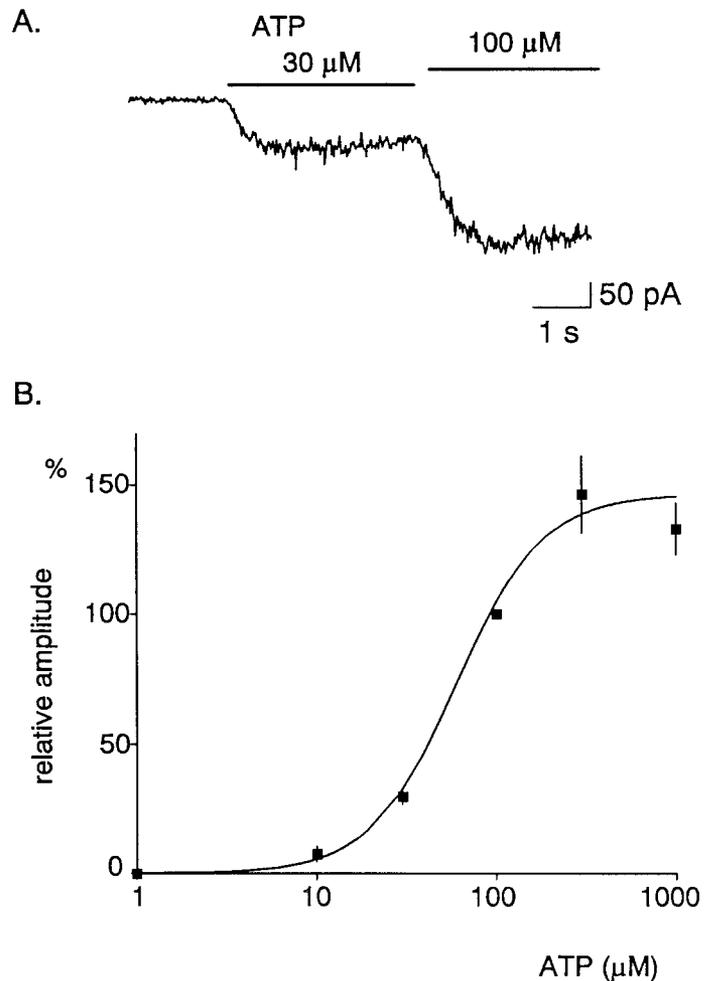
Figure 1. ATP-activated current in rat sympathetic neuron (*A*) and its concentration dependence (*B*). Holding potential was −80 mV. *A*, A typical recording of inward current activated by 30 and 100 μM extracellular ATP. *B*, Concentration–response relationship. The current activated by each concentration of ATP was normalized to the response at 100 μM in individual cells. Each symbol and bar represent mean and SEM from four to six cells tested. A sigmoidal curve was fitted to the data using a formula $I/I_{max} = A^n/[A^n + (EC_{50})^n]$, where *n* is a Hill coefficient, with $EC_{50} = 60$ μM, $n = 1.8$.

140 mM glucosamine hydrochloride was adjusted to pH 6.4 with 10 mM histidine so that glucosamine is >99% ionized (Benham and Tsien, 1987). No divalent cations or other materials were added to this solution. The solution containing Ca^{2+} as the only external cation was prepared with 2 mM $Ca(OH)_2$ as well as a desired concentration of $CaCl_2$, and pH was adjusted to 7.4 with HEPES (the final concentration of HEPES was about 5.4 mM). As for a 6 mM Ca^{2+} solution, 300 mM sucrose was also added for isotonicity.

All the experiments were performed at room temperature (about 22°C).

Drugs. Adenosine 5'-triphosphate disodium salt (ATP), acetylcholine chloride (ACh), α,β-methylene ATP tetralithium salt, hexamethonium chloride (C_6), and *d*-tubocurarine chloride [(+)-tubocurarine, d-TC] were from Sigma Chemical (St. Louis, MO). Suramin monosodium salt (Bayer, Leverkusen, Germany) was kindly supplied from Dr. K. Inoue of National Institute of Health Sciences, Japan.

Results

ATP-activated current in rat sympathetic neurons

ATP (100 μM) activated an inward current of several hundred picoamperes in isolated sympathetic neurons held at −60 mV (Fig. 1*A*). I_{ATP} was observed in practically all the cells tested

A.

B.
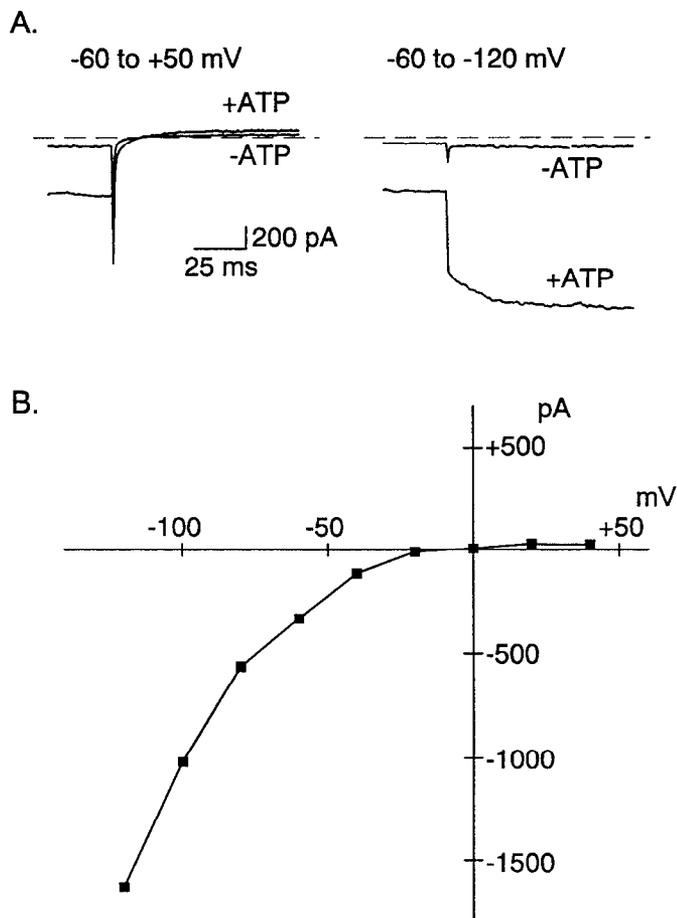
Figure 2. Voltage dependence of the ATP-activated current. *A*, The current responses recorded from a sympathetic neuron. A depolarizing step to +50 (*left*) or a hyperpolarizing step to −120 mV (*right*) was applied from a holding potential of −60 mV. The current traces before (−*ATP*) and during the application of 100 μM ATP (+*ATP*) were superimposed in each panel. *Broken lines* are zero-current levels. *B*, Current–voltage relationship obtained from another cell. The cell was held at −60 mV and a stepwise pulse decreasing from +40 mV to −120 mV with a 50 msec step duration was applied every 1 sec. The current at the end of each step was measured before and during the application of 100 μM ATP, and the difference was plotted against test potentials.

(>100 cells). For three cells that did not generate the ATP-activated current, I could not determine whether this was due to the nature of these cells or some improper experimental condition. The current activated by 100 μM ATP did not exhibit significant desensitization during application of several seconds. At higher concentration such as 1 mM, desensitization became evident (see Fig. 7*A*).

The concentration dependence of I_{ATP} was determined by applying multiple concentrations of ATP to same cells (Fig. 1). The experimental data could be fitted by a curve with EC_{50} of 60 μM and a Hill coefficient of 1.8 (Fig. 1*B*). The effect of α,β-methylene ATP was tested because the sensitivity to this compound was inconsistent among various types of neuronal cells (see Discussion). In three of three cells tested, α,β-methylene ATP (1 mM) did not activate an inward current.

Figure 2 shows the voltage dependence of I_{ATP} determined by applying stepwise pulses. I_{ATP} did not instantaneously reach steady state, but increased in a time-dependent manner upon strong hyperpolarization (Fig. 2*A*, right). I have not character-

A. ATP 100 μM

B. ATP 3 mM in Ca^{2+} 110 mM

-60 to -120 mV
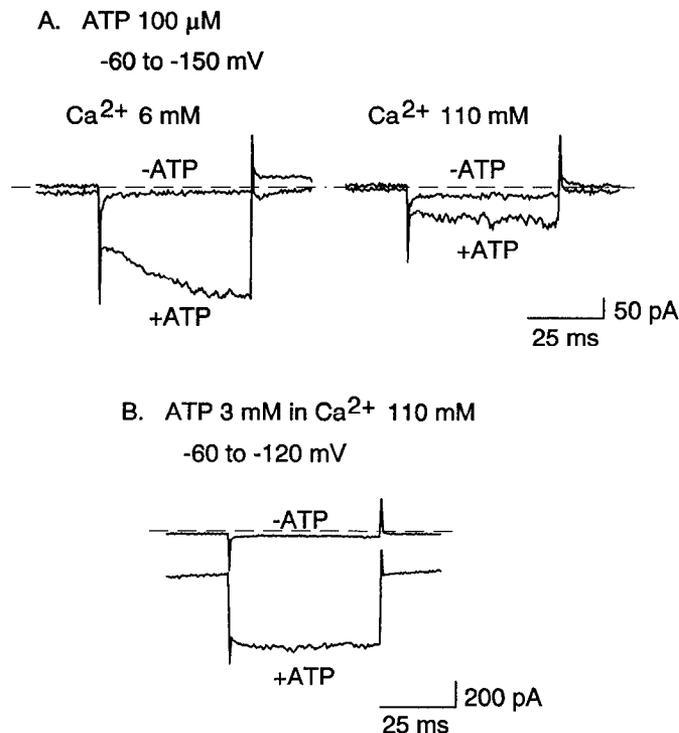
Figure 3. Current responses obtained with extracellular Ca^{2+} as the only extracellular cation. *Broken lines* are zero-current levels. *A*, Ca^{2+} current through the ATP-activated channels (*left*) and its reduction by high concentration of Ca^{2+} (*right*). A sympathetic neuron was exposed to a solution containing 6 mM $CaCl_2$ and 300 mM sucrose (*left*) or a solution containing 110 mM $CaCl_2$ (*right*), and then exposed to 100 μM ATP dissolved in each solution. The current in response to a hyperpolarizing step to −150 mV from a holding potential of −60 mV was recorded just before (−*ATP*) and during the exposure to ATP (+*ATP*), and the traces were superimposed in each panel. *B*, Induction of a large inward current by 3 mM ATP with 110 mM extracellular Ca^{2+}. The protocol was same as in *A*, except that a hyperpolarizing step to −120 mV was applied.

ized the time-dependent increase, but speculate that this might arise from voltage-dependent modulation of the ATP-activated channels similar to that reported for nicotinic receptor channels in skeletal muscle (Chabala, 1992). For the experiments to determine voltage dependence in this and following sections, the amplitude was measured at the end of 50–100 msec pulses when the current was regarded to have reached a steady state. I_{ATP} exhibited inward rectification and reversed around 0 mV (−6.1 ± 4.8 mV, mean ± SEM, n = 5). These properties are similar to those reported for I_{ATP} in various types of neuronal cells such as PC12 cells (Nakazawa et al., 1990b, 1991a), rat (Krishtal et al, 1988), or bullfrog (Bean et al., 1990) sensory neurons, and guinea pig sympathetic neurons (Evans et al., 1992). The reversal potential near 0 mV, combined with the finding that the current was much reduced when external Na^+ was replaced with sucrose or glucosamine (Fig. 3*A*; see Fig. 10*A*), suggests that I_{ATP} in rat sympathetic neurons is due to nonselective cation channels similar to those reported in other types of cells (see Bean and Friel, 1990).

Permeability to Ca^{2+} was tested using Ca^{2+} as the only external cation. With 6 mM $CaCl_2$ dissolved in an extracellular solution containing 300 mM sucrose, ATP (100 μM) activated a significant inward current (several hundred picoamperes at −150 mV; Fig. 3*A*, left). Thus, the ATP-activated channels in rat

sympathetic neurons are Ca^{2+} permeable as is the case of those in PC12 cells (Nakazawa et al, 1990b, 1991a), bullfrog sensory neurons (Bean et al., 1990), rat nucleus solitarius neurons (Ueno et al., 1992), and smooth muscle cells from rabbit ear artery (Benham and Tsien, 1987). The Ca^{2+} current activated by 100 μM ATP was, however, decreased when extracellular Ca^{2+} was increased from 6 mM to 110 mM (Fig. 3A, right). This accords with the phenomenon reported in PC12 cells (Nakazawa et al., 1990b). Honore et al. (1989) reported that reduction of I_{ATP} with high concentration of divalent cations was due to a decrease in the free-form of ATP, resulting from binding to these cations. A reduction of the effective concentration of ATP was also suggested by decreased single-channel openings with the higher concentration of divalent cations (Nakazawa and Hess, 1993). If this is the case, the current reduction should be overcome by increasing the concentration of ATP. A test was made by applying 3 mM ATP to cells bathed in 110 mM Ca^{2+}. As shown Figure 3B, a large current (several hundred picoamperes at -60 mV) was recorded in this condition. The result supports the idea that Ca^{2+} binds to ATP and reduces its effective concentration.

Lack of additivity of I_{ATP} *and* I_{ACh}

The currents activated by ACh have already been reported in mammalian sympathetic neurons (e.g., Derkach et al., 1983; Mathie et al., 1987). In the present study, ACh (10 μM to 1 mM), like ATP, activated an inward current in most cells (I_{ACh} was not observed only in 2 of >100 cells tested). The current activated by 100 μM ACh was three- to fivefold larger than that activated by 100 μM ATP in the same cells (see Fig. 5A). Unlike the current activated by 100 μM ATP (Fig. 1A), the current activated by 100 μM ACh exhibited significant inactivation; I_{ACh} was usually reduced to 40–70% of the peak amplitude in 2 sec during continuous exposure to ACh (see Fig. 5A, middle). Figure 4 shows the concentration and voltage dependence of I_{ACh}. The sensitivity of rat sympathetic neurons to ACh was similar to that to ATP: the concentration–response relationship could be fitted by a curve with an EC_{50} of 75 μM and a Hill coefficient of 2.2 (Fig. 4A). The voltage dependence of I_{ACh} exhibited inward rectification as reported previously (Mathie et al., 1987).
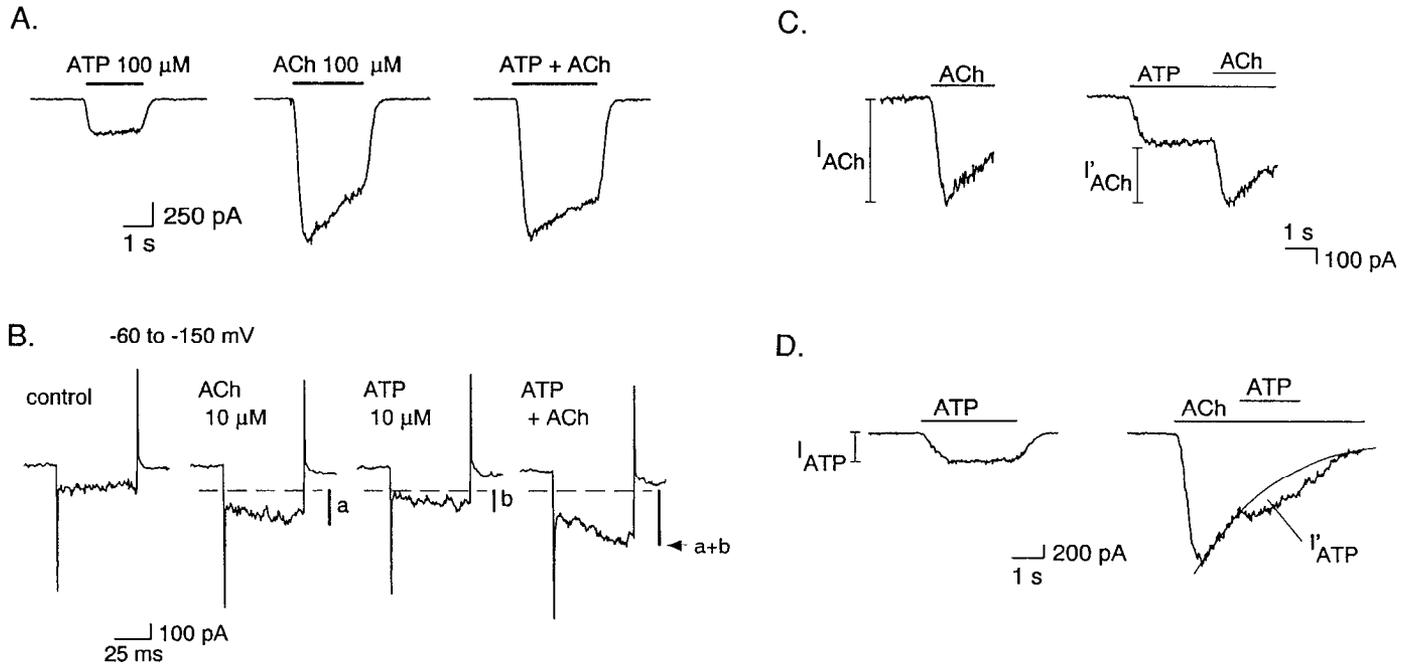
Figure 5 illustrates the currents activated by ATP, ACh, and their combined administration. ATP (100 μM) alone activated an inward current about one-fourth of the current activated by ACh (100 μM) in the cell shown in Figure 5A, but the combination of these agonists activated an inward current only as large as the current activated by ACh alone. In other words, ATP did not add any current to I_{ACh}. This "lack of additivity" was observed in five cells tested, and the current activated by ACh plus ATP was 99.8 ± 1.7% of the current activated by ACh alone (mean ± SEM). Although peak amplitude was not changed, desensitization of the current was significantly slowed in the presence of 100 μM ATP (Fig. 5A). For the cases where the cells were exposed to ACh with or without ATP longer than 2 sec, the current activated by ACh alone was decreased to 58.3 ± 3.1% of peak amplitude after 2 sec whereas the current activated by ACh and ATP was decreased to 70.3 ± 2.6% (n = 5). The difference was statistically significant (Student's t test, p < 0.05). In contrast to the data obtained with 100 μM concentrations of agonists, the current activated by 10 μM ATP and that by 10 μM ACh were additive in four of four cells tested (Fig. 5B).

A.

B. ACh 100 μM
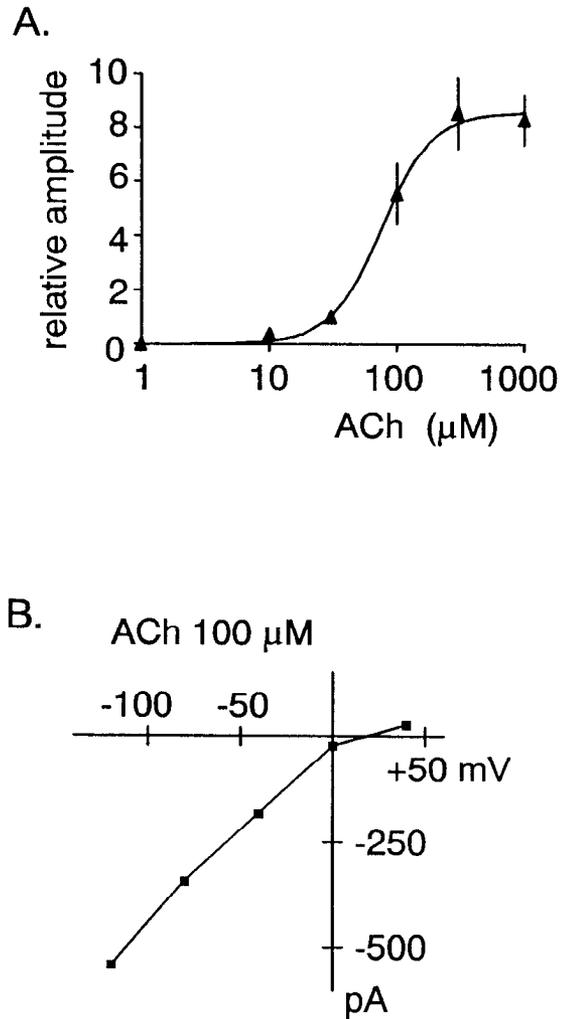
Figure 4. ACh-activated current in rat sympathetic neurons. *A*, Concentration dependence. Peak current amplitude obtained with various concentrations of ACh was normalized to the response at 30 μM in each cell. Each symbol and bar are mean and SEM from three to six cells held at -80 mV. The smooth curve was drawn as in Figure 1B with EC_{50} = 75 μM and n = 2.2. *B*, Current–voltage relation obtained from another cell. The current activated by 100 μM ACh was measured using a stepwise pulse as in Figure 2B.

The additivity of the two currents activated by 100 μM concentrations of agonists was also assessed by comparing I_{ATP} before and during the ATP application (Fig. 5C). The mean amplitude of I_{ATP} was 31.9 ± 3.4% of I_{ACh} (mean ± SEM, n = 10) in this series of experiments. The current activated by ACh in the presence of I_{ATP} (Fig. 5C, right; I'_{ACh}) was always about 30–40% smaller than that activated in the absence of I_{ATP} (67.7 ± 3.2% of ACh alone, n = 10), suggesting again that two currents are not additive. The opposite, that is, the reduction of I_{ATP} during the ACh application, was also observed (Fig. 5D). The mean ATP-activated current in the presence of ACh was 39.7 ± 10.7% of that in the absence of ACh (n = 6).

Figure 6 illustrates the effects of suramin, a P_2-purinoceptor antagonist (Dunn and Blakely, 1988; Nakazawa et al., 1990a, 1991b), on I_{ATP} and I_{ACh}. I_{ATP} was reversibly antagonized by 100 μM suramin (Fig. 6A) whereas I_{ACh} was not affected (Fig. 6B). When I_{ATP} was partially inhibited by 300 μM suramin, the inhibition by 100 μM ATP of I_{ACh} was attenuated (Fig. 6C,D). The

A.

ATP 100 µM   ACh 100 µM   ATP + ACh

_| 250 pA
1 s

C.

ACh   ATP ACh

I_{ACh} I'_{ACh}

1 s
⌐ 100 pA

B.   -60 to -150 mV

control   ACh 10 µM   ATP 10 µM   ATP + ACh

|a |b   ◄ a+b

_| 100 pA
25 ms

D.

ATP   ATP
           ACh

I_{ATP} I'_{ATP}

_| 200 pA
1 s

Figure 5. Test of additivity of the ATP- and the ACh-activated currents. *A*, The lack of additivity the current activated by 100 µM ATP and that by 100 µM ACh. A cell was held at −80 mV, and ATP, ACh, and ATP plus ACh were applied successively with an interval of 40 sec (*left to right*). Note that the amplitude of the current activated by ATP plus ACh (*right*) was not different from that by ACh alone (*middle*). *B*, Additivity of the currents activated by 10 µM ATP and by 10 µM ACh recorded from another cell. The protocol was same as in *A*, except that a hyperpolarization pulse to −150 mV was applied every 1 sec during the application of the agonists. *Broken lines* indicate current levels at −150 mV just before the agonist application (practically same as the trace shown as control). The current activated by ATP plus ACh (*right*) agreed with the value (indicated with an *arrow*) that is the sum of the currents activated by each agonist (*vertical bars with a or b*). *C*, Decrease in the ACh (100 µM)-activated current in the presence of the current activated by ATP (100 µM). Holding potential was −80 mV. The ACh-activated current during the ATP application (I'_{ACh}, *right*) was about 40% smaller than control current (I_{ACh}, *left*) in this case. *D*, Decrease in the ATP (100 µM)-activated current in the presence of the current activated by ACh (100 µM). Holding potential was −80 mV. The current activated by ATP in the presence of ACh (I'_{ATP}, *right*) was about 40% of control current (I_{ATP}, *left*) in this case.

results suggest that the inhibition as well as the channel activation by ATP is mediated though P_2-purinoceptors.

Figure 7 shows repeated activation of I_{ATP} and I_{ACh} during continuous application of the other agonist. In these experiments, 1 mM concentrations of the agonists were continuously superfused to induce complete desensitization. ATP (100 µM), applied immediately after activation of I_{ACh}, did not produce any change in the current trace (Fig. 7*A*, left), but it did activate an additional current when I_{ACh} was considerably inactivated (Fig. 7*A*, right). The results suggest that the opening of the ACh-activated channels, but not the presence of ACh itself, is responsible for the inhibition of I_{ATP}. The opposite case, that is, the requirement of the opening of the ATP-activated channels for the inhibition of I_{ACh}, was also indicated as shown in Figure 7*B*; the additional current activated by 100 µM ACh, applied after significant inactivation of I_{ATP}, was larger compared with the response immediately after the activation of I_{ATP}. Similar results were obtained in four of four cells tested for each agonist.

Effects of open-channel blockers of nicotinic receptor channels

It has been demonstrated that a subclass of nicotinic receptor channel antagonists including hexamethonium (C_6) and *d*-tubocurarine (d-TC) inhibits ion permeation mainly or entirely by acting on the open-state of the channels in *Aplysia* neurons (Marty et al., 1976; Ascher et al., 1978) and rat parasympathetic ganglion cells (Ascher et al., 1979). In addition, the reduction of the ATP-activated current in the presence of high concentrations of d-TC also exhibited characteristics of the open-chan-
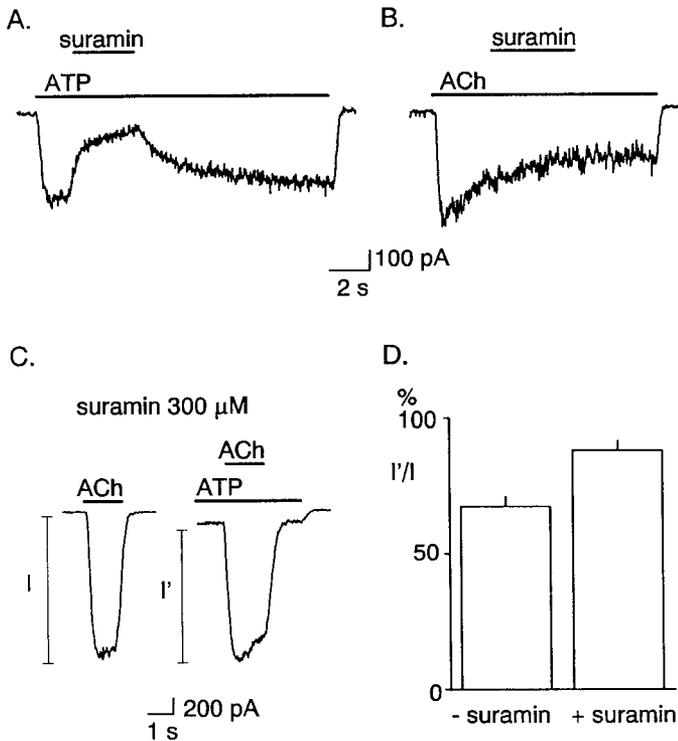
nel block in PC12 cells (Nakazawa et al., 1991b). I investigated the effects of these open-channel blockers on I_{ATP} and I_{ACh}.

C_6 or d-TC inhibited I_{ACh} (Fig. 8) in a concentration range similar to that reported in rat parasympathetic neurons (Ascher et al., 1979). In contrast to I_{ACh}, I_{ATP} was only slightly inhibited by 100 µM C_6 (Fig. 8*B*,*D*). d-TC (100 µM) strongly blocked I_{ATP}, but sensitivity of I_{ATP} to d-TC was considerably less than that of I_{ACh} (Fig. 8*B*,*C*). The results show that these open-channel blockers distinguish between I_{ATP} and I_{ACh}.

The additivity of the two types of currents was tested in the presence of these open-channel blockers. The reduction by ATP of I_{ACh} measured after partial current blockade by 1 µM d-TC or 10 µM C_6 was not different from that measured without the blockers (Fig. 9*A*,*B*), suggesting that the blockers do not affect the sensitivity of I_{ACh} to ATP. In contrast, the reduction by ACh of I_{ATP} was much relieved after the blockade of I_{ACh} (Fig. 9*C*,*D*).

Permeability of glucosamine

Purinoceptor-mediated conductance was more permeable to cations of large molecular weight than nicotinic receptor-mediated conductance in PC12 cells (Nakazawa et al., 1991a). I examined whether such different permeability is observed with glucosamine between the ATP- and the ACh-activated conductance (Fig. 10). With 140 mM extracellular glucosamine, ATP (100 µM) activated an inward current of about 50 pA at −150 mV (Fig. 10*A*, left) whereas ACh (100 µM) activated only a small current (<10 pA at −150 mV) in the same cell (Fig. 10*A*, right). I_{ACh} measured with glucosamine was 10–20% of I_{ATP} at −150

Figure 7. Repetitive application of 100 μM ATP (*A*) or ACh (*B*) during desensitization of the current activated by a high concentration (1 mM) of the other agonist. *A* and *B* were obtained from a cell held at -80 mV.

Figure 6. Influence of suramin on current response. Holding potential was -80 mV. *A* and *B*, Selective block by suramin of the ATP-activated current. Suramin (100 μM) was applied to a sympathetic neuron while the current activated by 100 μM ATP (*A*) or 30 μM ACh (*B*) persisted. *C*, Relief by suramin of the ATP (100 μM)-induced inhibition of the ACh (100 μM)-activated current. The protocol was same as in Figure 5*C*, except that suramin (300 mM) was applied 10 sec before and was present throughout the exposure to ACh. *D*, Comparison of the ratio of the ACh-activated current with or without suramin. The current ratio (I'/I) was obtained as shown in *C*. Each column represents 10 ($-suramin$) or 4 ($+suramin$) cells tested. Bars are SEM.

mV in six cells tested. Although the result is most likely explained by greater permeation of glucosamine through the ATP-activated conductance than that through the ACh-activated conductance, another explanation is also possible, that is, the inhibition by glucosamine of the ACh-binding to nicotinic receptor channels. This is expected because both ACh and glucosamine have a positively charged nitrogen in their chemical structures. Tests were therefore made to examine whether glucosamine affects the ACh binding. First, a high concentration (3 mM) of ACh was applied in the presence of 140 mM glucosamine. I_{ACh} was also small in this condition (Fig. 10*B*). Second, ACh (100 μM) was applied in the presence of 70 mM glucosamine as well as 70 mM Na$^+$ as a permeable cation. This was designed to test a possibility that the binding of 3 mM ACh was completely blocked by 140 mM glucosamine in the experiment shown in Figure 10*B*. If glucosamine exerts such strong inhibition on the ACh binding, a 70 mM concentration of this compound is sufficient to abolish the response induced by 100 μM ACh. In contrast to this speculation, ACh (100 μM) activated a significant inward current (Fig. 10*C*). The appearance of I_{ACh} in this condition also excludes a possibility that the acidic condition (pH 6.4) employed for the experiments with glucosamine (see Materials and Methods) reduced the response to ACh because the experiment shown in Figure 10*C* was performed at pH 6.4. The very small current with ACh can thus be best interpreted as
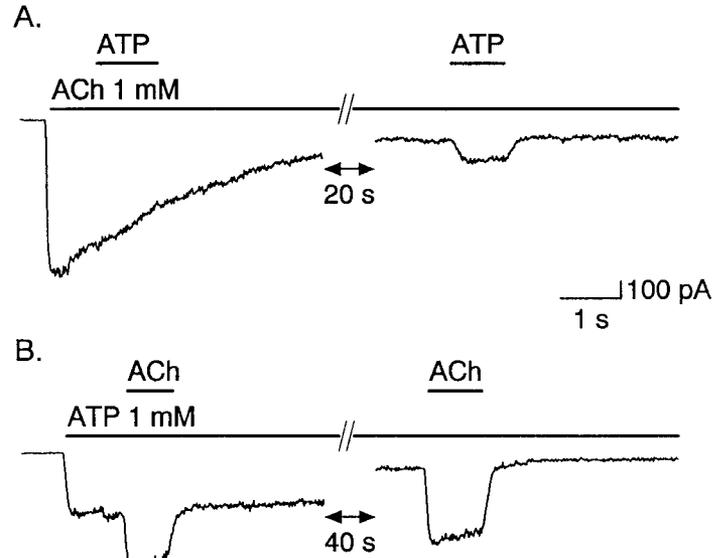
poor permeation of glucosamine through the ACh-activated channels.

With extracellular glucosamine, ACh simultaneously applied with ATP reduced I_{ATP} (Fig. 11). The reduction was observed in five of five cells tested, and the mean reduction was 23 $\pm$ 5% of I_{ATP} in the absence of ACh (mean $\pm$ SEM).

Discussion

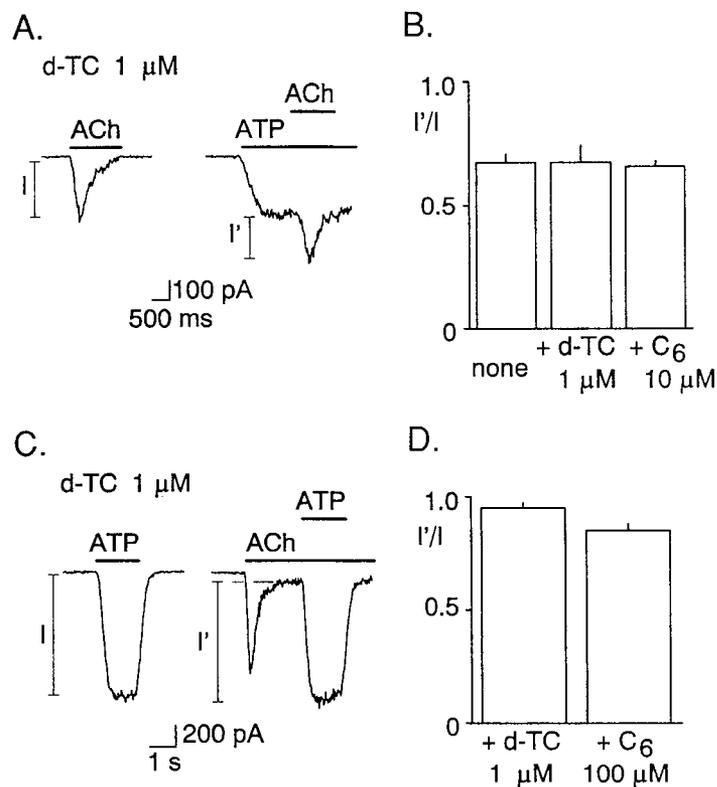*Properties of ATP-activated channels in rat sympathetic neurons*

Almost all the cells ($>97\%$) responded exogenous ATP in rat sympathetic neurons. This proportion of cells responsive to ATP is as large as that reported in cultured sympathetic neurons isolated from guinea pig celiac ganglia ($>95\%$; Evans et al., 1992), and higher than that reported in parasympathetic neurons isolated from guinea pig cardiac ganglia ($\sim75\%$; Fieber and Adams, 1991). On the other hand, only a minority of cells responded to ATP in rat and bullfrog sensory neurons (Bean, 1990).

The ATP-activated channels are cation selective but have poor selectivity among cation species, which is a common feature of the channels in this group regardless of types of cells (Bean and Friel, 1990; Bean, 1992). Other properties of these channels, such as voltage dependence at positive potential, single-channel conductance, or pharmacology, are not necessarily common features. Compared with the ATP-activated channels in other types of neuronal and non-neuronal cells, the channels in rat sympathetic neurons are characterized as follows. (1) The channels in rat sympathetic neurons, like those in PC12 cells (Nakazawa et al., 1991a,b) or rat solitarii neurons (Ueno et al., 1992), exhibit EC$_{50}$ values around 50 μM for ATP (Fig. 1*B*), while the channels in rat and frog sensory neurons (Bean, 1990) or cultured guinea pig sympathetic neurons (celiac ganglia; Evans et al., 1992) have higher sensitivity to ATP (EC$_{50}$ < 10 μM). (2) The current–voltage relationship for the ATP-activated current in rat sympathetic neurons (Fig. 2*B*) exhibited inward rectification as is the case for the currents reported in all of the neu-
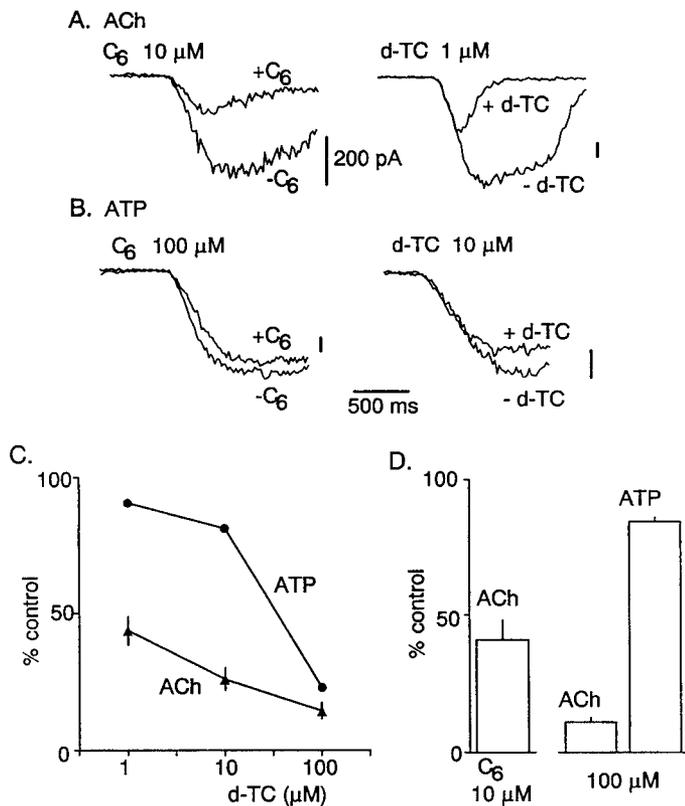
Figure 8. Selective block by hexamethonium (C_6) and d-tubocurarine (d-TC) of the ACh-activated current. The current was activated by 100 μM of each agonist. For the traces with C_6 and d-TC, the blockers were only present during agonist application. Holding potential was −80 mV. *A* and *B,* Superimposed current traces recorded with or without the blockers. Each panel illustrates data obtained from four different cells. The ACh-activated current was largely suppressed by 1 μM C_6 or 10 μM d-TC (*A*) whereas the reduction in the ATP-activated current was small even with a 10-fold higher concentration of each blocker (*B*). *C* and *D,* Summarized data of selective block by d-TC (*C*) or C_6 (*D*). Peak amplitude with each blocker was normalized to that without blockers. Each symbol or column represents the mean from four to five cells tested. Bars are SEM.

Figure 9. *A* and *B,* Test of additivity of the currents activated by 100 μM ATP and 100 μM ACh in the presence of open-channel blockers. The protocol was same as in Figure 5C, except that d-TC (1 μM) or C_6 (10 μM) was applied 10 sec before and was presented during the ACh application. The current ratio (*I'/I*) was obtained as shown in *A,* and compared with the ratio without blockers in *B.* Each column and bar represent the mean and SEM from 10 (*none*) or 5 (*d-TC* or C_6) cells tested. *C* and *D,* Activation by ATP of the channels first inhibited by open-channel blockers. The protocol was the same as in *A,* except that the order of the application of ATP (100 μM) and ACh (100 μM) was opposite. A typical response obtained with 1 μM d-TC (*C*) and summarized data from four (*d-TC,* 1 μM) or five (C_6, 100 μM) cells tested (*D*). Each column and bar in *D* are mean and SEM.
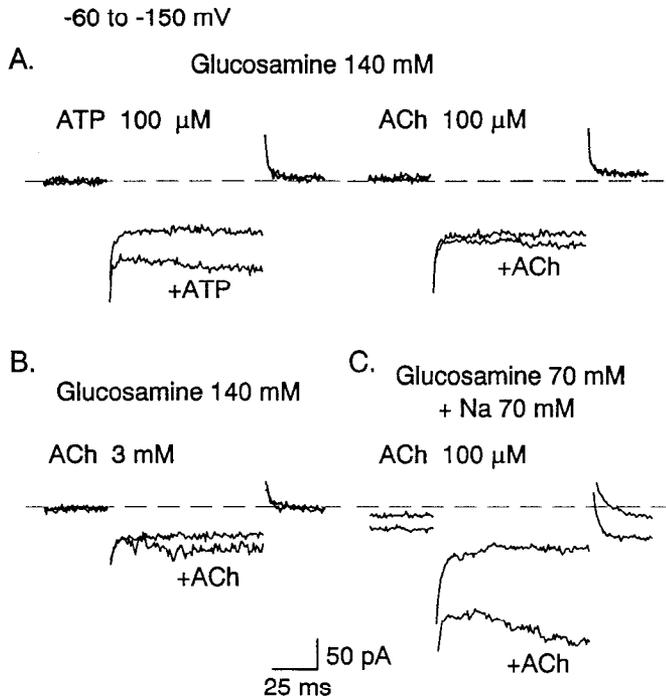
ronal cells listed above, unlike the current in frog cardiac cells (Friel and Bean, 1988) or smooth muscle cells from rat myometrium (Honore et al., 1989). (3) α,β-Methylene ATP was inactive in rat sympathetic neurons, as in PC12 cells (Nakazawa et al., 1990b), rat parasympathetic neurons (Fieber and Adams, 1991), or rat solitarii neurons (Ueno et al., 1992), whereas this compound is a potent agonist to activate an inward current in guinea pig sympathetic neurons (Evans et al., 1992) or smooth muscle cells from rabbit ear artery (Benham and Tsien, 1987). From these comparisons, it is concluded that the properties of the ATP-activated channels mostly resemble those in PC12 cells among "ATP-activated channel family" reported to date. This finding is not surprising because (1) PC12 cells are derived from a rat adrenal pheochromocytoma cell (Greene and Tischler, 1976), and they must have genetic similarity with other rat cells; and (2) PC12 cells, which are originated from a rat adrenal medullary cell, retain well a fundamental function in common with sympathetic neurons, namely, the release of catecholamines upon nicotinic ACh stimulation (e.g., Inoue and Kenimer, 1988). Perhaps the properties of the ATP-activated channels vary depending on both species and types of tissues, as indicated from the difference in sensitivity to ATP or α,β-methylene ATP

between rat sympathetic neurons reported here and guinea pig sympathetic neurons (Evans et al., 1992), or rat sensory neurons (Bean, 1990).

Another similarity between the ATP-activated current in rat sympathetic neurons and that in PC12 cells is that the current is "apparently" blocked by high concentrations of Ca^{2+} (Fig. 3*A;* Nakazawa et al., 1991a). A similar "apparent" block was also reported for the ATP-activated current in rat myometrial smooth muscle cells (Honore et al., 1989). The "apparent" blockade was not observed in rat and frog sensory neurons (Bean, 1990) or smooth muscle cells from rabbit ear artery (Benham and Tsien, 1987); ATP (10–100 μM) activated a large inward current even with isotonic extracellular Ca^{2+} in these cells. As compared above, rat sympathetic neurons and PC12 cells exhibited low sensitivity to ATP ($EC_{50} \sim 60$ μM). Rat myometrial smooth muscle cells also showed low sensitivity to ATP (EC_{50} of 660 μM; Honore et al., 1989). On the other hand, rat and frog sensory neurons and smooth muscle cells from rabbit ear artery appear to have high sensitivity to ATP because a significant current was observed with 1 μM ATP (Benham and Tsien, 1987; Bean, 1990). Thus, the reduction by high concentration of Ca^{2+} may be restricted to the channels of low affinity
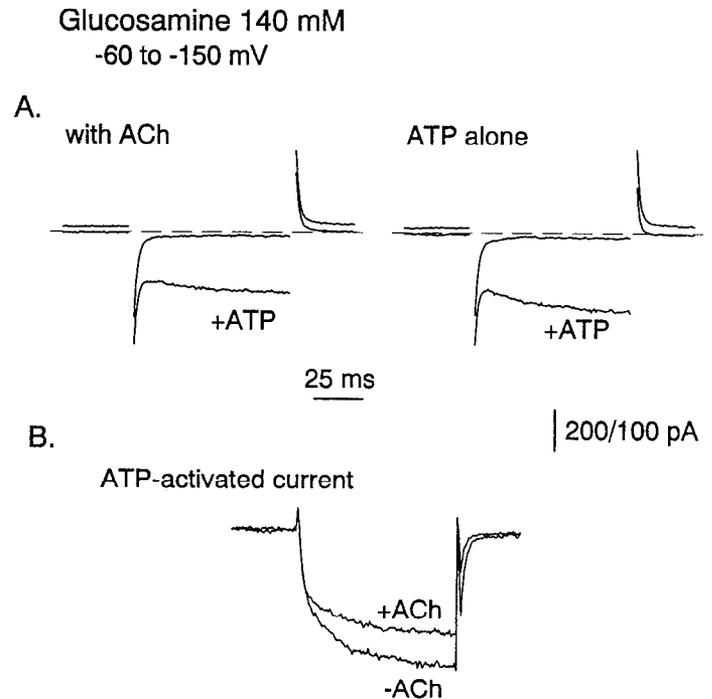
-60 to -150 mV

A.

Glucosamine 140 mM

ATP 100 μM   ACh 100 μM

+ATP   +ACh

B.
Glucosamine 140 mM

C. Glucosamine 70 mM
   + Na 70 mM

ACh 3 mM   ACh 100 μM

+ACh

+ACh

‾‾|50 pA
25 ms

Figure 10. Selective permeation of glucosamine to the ATP-activated conductance. The cells were held at −60 mV and a hyperpolarizing step to −150 mV was applied every 1 sec. Each panel illustrates superimposed traces of the current just before and during the agonist application. *Broken lines* are zero-current levels. *A,* The appearance of a significant inward current upon ATP (100 μM) application (*left*), but not upon ACh (100 μM) application (*right*), to a cell bathed in extracellular solution containing 140 mM glucosamine. *B,* Lack of current induction by a high concentration (1 mM) of ACh with 140 mM extracellular glucosamine. *C,* Induction by 100 μM ACh of a large inward current in a cell bathed in solution containing 70 mM glucosamine and 70 mM Na$^+$. pH of this solution was adjusted to 6.4 with 10 mM histidine as is the case of 140 mM glucosamine solution (see Materials and Methods).

to ATP. Assuming that effective concentration of ATP is reduced by its binding to Ca^{2+}, the difference among these channels in regard to the block by Ca^{2+} may be explained by movement of ATP between Ca^{2+} and the ATP-binding site on the channels. Negatively charged ATP may interact with the high-affinity binding site, but not with the low-affinity binding site, strongly enough to be deprived from Ca^{2+}. Another explanation for this diversity in sensitivity to Ca^{2+} is different allosteric effects of Ca^{2+} on the receptors to ATP.

Negative interaction between I$_{ATP}$ *and* I$_{ACh}$

The current activated by 100 μM ATP and that by 100 μM ACh were not additive (Fig. 5). This phenomenon may not require slow second messengers because the lack of additivity was observed very rapidly with simultaneous application of ATP and ACh (Fig. 5*A*). The lack of additivity appears to be related directly to channel opening, since the ATP- or the ACh-activated component was increased when the current activated by the other agonist was desensitized (Fig. 7). Thus, the phenomenon is most likely explained by the existence of a population of channels that are activated by both ATP and ACh, as was suggested for the lack of additivity of the current activated by ATP and that by nicotine in PC12 cells (Nakazawa et al., 1991a). In other words, populations of these two types of ligand-gated channels may be overlapped. Another possibility of a contri-

Glucosamine 140 mM
-60 to -150 mV

A.

with ACh   ATP alone

+ATP   +ATP

25 ms

B. |200/100 pA

ATP-activated current

+ACh

-ACh

Figure 11. *A,* Reduction by ACh of glucosamine influx through the ATP-activated channels. The cell bathed in 140 mM glucosamine was first exposed simultaneously to 100 μM ATP and 100 μM ACh (*left*), and, after a 40 sec rinse, exposed to 100 μM ATP alone (*right*). The current traces just before and during the application were superimposed in each panel. Note that the inward current activated by ATP alone (*right*) was larger than the current in the presence of ACh (*left*). *Broken lines* are zero-current levels. *B,* Glucosamine influx through the ATP-activated channels in the presence and absence of ACh. The differences in the current traces in each panel of *A* were superimposed.

bution by some very rapid blocking mechanisms such as those resulting from "membrane-delimited" modulation of channels (Hille, 1992c) is, however, not excluded at present.

Another possible mechanism underlying the negative interaction is channel inhibition by intracellular Ca^{2+}. The idea is that Ca^{2+} (or other divalent cations) flowing through the ACh-activated channels inactivates the ATP-activated channels and vice versa. This was expected because Ca^{2+} is permeant to both neuronal nicotinic receptor channels (Vernino et al., 1992) and the ATP-activated channels (Bean et al., 1990; Nakazawa et al., 1990). Na$^+$ influx through the ATP-activated channels was blocked by intracellular Ca^{2+} in PC12 cells (Nakazawa and Hess, 1993). As for nicotinic receptor channels, blockade by intracellular Mg^{2+} of Na$^+$ permeation was also reported in PC12 cells (Ifune and Seinbach, 1991). However, the block by Ca^{2+} (or Mg^{2+}) flowing through the channels may not be the cause for the negative interaction reported here because (1) the block by ACh of the ATP-induced glucosamine influx (Fig. 11) was obtained in the absence of divalent cations, and (2) the ACh- and the ATP-activated currents were not additive even in divalent cation-free extracellular solution containing 140 mM NaCl in PC12 cells (K. Nakazawa, unpublished observation).
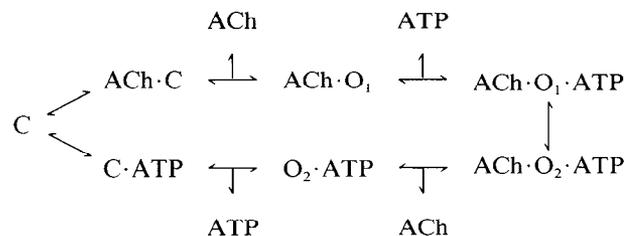
Explanation for properties of the current interaction based upon the "channel overlap"

ATP (100 μM) did not add current to the current activated by 100 μM ACh (Fig. 5*A*). Based on the hypothesis of "channel

overlap," this result suggests that most of the channels sensitive to ATP are activated by 100 μM ACh. In other words, the population of the channels activated by ATP is almost completely involved in the population of the nicotinic receptor channels in the rat sympathetic neurons. Another explanation is that a considerable number of "ACh-insensitive" ATP-activated channels exist in these cells, but this component is not observed. If the "ATP-sensitive" ACh-activated channels are led to different open states by two agonists and the ATP-induced state has smaller conductance (see below), shift from the ACh-induced state to the ATP-induced state in the presence of ATP may result in reduction of a current component mediated by these channels. This current reduction may mask an additional current component mediated by "ACh-insensitive" ATP-activated channels. On the other hand, the currents activated by a low concentration (10 μM) of each agonist were additive (Fig. 5B). This can be explained by small occupancy of the receptors to each agonist. The receptor occupancy with 10 mM of each agonist may be less than 10%, judging from concentration–response relationship (Figs. 1B, 4A). Thus, even if ATP and ACh activate a completely common population of channels, the channels activated by this concentration of agonists may not be largely overlapped with each other.

The selective inhibition by the open-channel blockers of the ACh-activated current (Fig. 8) can be interpreted in two different ways. One interpretation is discrimination of open states; the open-channel blockers may selectively inhibit the open state induced by ACh whether the channels are ATP sensitive or not. The other is discrimination of the channels; the "ATP-sensitive" and the "ATP-insensitive" ACh-activated channels may have different sensitivity to the open-channel blockers, and the blockers may preferentially block the "ATP-insensitive" channels. The extent of the reduction by ATP of I_{ACh} obtained after the partial channel blockade of I_{ACh} was not different from that obtained without channel blockade (Fig. 9A,B). This result indicates that the channels are equally inhibited whether they are ATP sensitive or not, and supports the idea that the open-channel blockers discriminate the open state induced by ACh and that by ATP. Thus, for the "ATP-sensitive" ACh-activated channels, these channels may be led to different open states by ACh and ATP. The diversity of the open states of the "ATP-sensitive" ACh-activated channels is also supported by different permeability of cations of glucosamine (Fig. 10). In preliminary experiments, ATP activated single-channel currents of amplitude (about 1.3 pA at −80 mV) smaller than that activated by ACh (about 3 pA at −80 mV) in the same outside-out membrane patches excised from the rat sympathetic neurons (Nakazawa, unpublished observation). This finding accords with the idea of different open states, though I have not determined whether or not the different amplitude arises from channel activity of the same channels. In contrast, both agonists appear to induce the same open state in skeletal muscle cells, judging from single-channel currents (Kolb and Wakelam, 1983; Igusa, 1988) and sensitivity to d-TC (Igusa, 1988). The "ATP-sensitive" ACh-activated channels in these skeletal muscle cells may stay at similar open states upon activation by either ATP or ACh.

I describe below a kinetic model for the behavior of the "ATP-sensitive" ACh-activated channels to provide better understanding of the hypothesis, as we proposed for a similar interaction in PC12 cells (Nakazawa et al., 1991a). The model is as follows:

$$
\begin{array}{ccccc}
& \mathrm{ACh} & & \mathrm{ATP} & \\
& \mathrm{ACh \cdot C} \xrightarrow{} & \mathrm{ACh \cdot O_1} \xrightarrow{} & \mathrm{ACh \cdot O_1 \cdot ATP} \\
\mathrm{C} & & & \uparrow \\
& \mathrm{C \cdot ATP} \xrightarrow{} & \mathrm{O_2 \cdot ATP} \xrightarrow{} & \mathrm{ACh \cdot O_2 \cdot ATP} \\
& \mathrm{ATP} & & \mathrm{ACh} &
\end{array}
$$

where C is a closed state, and O_1 or O_2 is an open state induced by ACh or ATP, respectively. In this model, different binding sites were assumed for ACh and ATP because suramin selectively inhibited I_{ATP} (Fig. 6A). The reduction by ACh of the ATP-induced glucosamine influx is explained by the shift of a part of channels from the ATP-induced "glucosamine-permeable state" to the ACh-induced "glucosamine-impermeable state" via a route, $O_2 \cdot ATP — ACh \cdot O_2 \cdot ATP — ACh \cdot O_1 \cdot ATP$ in the scheme above.

With the open-channel blockers, I_{ATP} in the presence of ACh, measured after significant inhibition by the blockers of I_{ACh}, was comparable to I_{ATP} in the absence of ACh (Fig. 9C,D). This indicates that activation by ATP of "ATP-sensitive" ACh-activated channels was not affected by the blockers. ATP may rapidly "unblock" the channels that have been blocked by d-TC or C_6.

Molecular basis of "the channel overlap"

A line of evidence has suggested that each member of the ligand-gated channel superfamily contains five subunits (Betz, 1990; Hille, 1992a). As the ATP-activated channel appears to be a member of this superfamily, judging from its fast activation kinetics, the lack of requirement of soluble cellular component, and ion selectivity similar to that of other cation-selective ligand-gated channels (see review, Bean and Friel, 1990), it seems reasonable to hypothesize that this channel also consists of five subunits. With this expectation, two simple models for molecular basis of the overlap of the ATP- and the ACh-activated channels can be proposed. One is the existence of a subunit containing both the ACh- and the ATP-binding sites, that is, the idea that an ACh-binding (α) subunit also binds to ATP. The other is "heterometric" assembly of the ACh binding and the ATP-binding subunits (Bean, 1992); the ATP binding protein may form "heterometric" channels with the ACh-binding or nonbinding ($n\alpha$) subunits of the nicotinic receptor channels. In either of these two cases, the similarity between the ATP-binding subunit and the subunits of nicotinic receptor channels is expected. Such similarity is supported, at least, by estimation of the size of the ATP-binding protein. The molecular weight of the ATP-binding protein was estimated to be 53 kDa in PC12 cells (Majid et al., 1992), which is close to those of the subunits of the nicotinic receptor channels (Hille, 1992a). A similar value (62 kDa) was reported for an ATP-binding protein isolated from rat vas deferens (Bo et al., 1992), where the ATP-activated channels also exist (Nakazawa and Matsuki, 1987; Friel, 1988).

Physiological significance of interaction between ATP- and ACh-activated channels

A detailed concept of "cotransmitters" has been discussed by Burnstock (1990b). The most popular cotransmission including ATP is that observed in sympathetic nerve terminals in smooth muscle tissues. ATP and noradrenaline are believed to be released from the same terminals and synergistically activate

smooth muscle contraction, although the mechanism underlying the induction of contraction may be completely different between these transmitters (Burnstock, 1990a,b). Similar synergistic cotransmission by ACh and ATP may occur in postsynaptic neurons of sympathetic ganglia because ACh, like noradrenaline, is stored with ATP in nerve terminals (Burnstock, 1990b). The expected synergistic cotransmission must result from a similar mechanism, namely, the activation of cation-selective channels. As almost all the cells responded to both ACh and ATP in the present study, the possibility of such synergetic transmission appears to be very high. In addition, based upon the hypothesis of activation by ATP of a subpopulation of nicotinic receptor channels, sympathetic neurons can modulate their sensitivity to these transmitters by regulating the numbers of the ATP-sensitive and the ATP-insensitive channels. Such regulation enables the cells to exhibit heterogeneous responsiveness even if the released transmitters are identical. The idea of activation by cotransmitters of a common population of channels may, thus, provide a novel view for modulation of neurotransmission at postsynaptic membrane.

Conclusion

ACh, an established excitatory neurotransmitter, and ATP, a candidate for an excitatory neurotransmitter, reciprocally inhibited the current activated by the other agonist in rat sympathetic neurons. The hypothesis of a common population of channels that are led to different open states by ATP and ACh can explain the negative interaction and the heterogeneous properties of the ACh- and the ATP-induced conductance. This report for the first time demonstrates "nonindependence" of the ACh- and the ATP-activated channels in neurons. A similar relation may also exist in both peripheral (Bean, 1990; Fieber and Adams, 1991; Evans et al., 1992) and central (Edwards et al., 1992) neurons, where both purinoceptor and nicotinic receptor agonists activate ionic currents.

References

Ascher P, Marty A, Neild TO (1978) The mode of action of antagonists of the excitatory response to acetylcholine in *Aplysia* neurons. J Physiol (Lond) 278:177–206.

Ascher P, Large WA, Rang HP (1979) Studies on the mechanism of action of acetylcholine antagonists on rat parasympathetic ganglion cells. J Physiol (Lond) 295:139–170.

Bean BP (1990) ATP-activated channels in rat and bullfrog sensory neurons: concentration dependence and kinetics. J Neurosci 10:1–10.

Bean BP (1992) Pharmacology and electrophysiology of ATP-activated ion channels. Trends Pharmacol Sci 13:87–90.

Bean BP, Friel DD (1990) ATP-activated channels in excitable cells. In: Ion channels, Vol 2 (Narahashi T, ed), pp 288–321. New York: Plenum.

Bean BP, Williams CA, Ceelen PW (1990) ATP-activated channels in rat and bullfrog sensory neurons: current–voltage relation and single channel behavior. J Neurosci 10:11–19.

Benham CD (1989) ATP-activated channels gate calcium entry in single smooth muscle cells dissociated from rabbit ear artery. J Physiol (Lond) 419:689–701.

Benham CD, Tsien RW (1987) A novel receptor-operated Ca^{2+}-permeable channel activated by ATP in smooth muscle. Nature 328:275–278.

Betz H (1990) Ligand-gated ion channels in the brain: the amino acid receptor superfamily. Neuron 5:383–392.

Bo X, Simon J, Burnstock G, Barnard EA (1992) Solubilization and molecular size determination of the P_{2x} purinoceptor from rat vas deferens. J Biol Chem 267:17581–17587.

Burnstock G (1990a) Noradrenaline and ATP as cotransmitters in sympathetic nerves. Neurochem Int 17:357–368.

Burnstock G (1990b) Co-transmission. Arch Int Pharmacodyn Ther 304:7–33.

Burnstock G, Kennedy C (1985) A dual function for adenosine 5'-triphosphate in the regulation of vascular tone: excitatory cotransmitter with noradrenaline from perivascular nerves and locally released inhibitory intravascular agent. Circ Res 58:319–330.

Chabala LD (1992) Voltage dependence of acetylcholine receptor channel gating in rat myoballs. J Gen Physiol 100:729–748.

Derkach VA, Selyanko AA, Skok VI (1983) Acetylcholine-induced current fluctuations and fast excitatory post-synaptic currents in rabbit sympathetic neurones. J Physiol (Lond) 336:511–526.

Dunn PM, Blakely AGH (1988) Suramin: a reversible P_2-purinoceptor antagonist in the mouse vas deferens. Br J Pharmacol 93:243–245.

Edwards FA, Gibb AJ, Colquhoun D (1992) ATP receptor-mediated synaptic currents in the central nervous system. Nature 359:144–147.

Evans RJ, Derkach V, Surprenant A (1992) ATP mediates fast synaptic transmission in mammalian neurons. Nature 357:503–505.

Fieber L, Adams DJ (1991) Adenosine triphosphate-evoked currents in cultured neurons dissociated from rat parasympathetic cardiac ganglia. J Physiol (Lond) 434:239–256.

Friel DD (1988) An ATP-sensitive conductance in single smooth muscle cells from the rat vas deferens. J Physiol (Lond) 401:361–380.

Friel DD, Bean BP (1988) Two ATP-activated conductances in bullfrog atrial cells. J Gen Physiol 91:1–27.

Greene LA, Tischler AS (1976) Establishment of a noradrenergic clonal line of rat adrenal pheochromocytoma cells which respond to nerve growth factor. Proc Natl Acad Sci USA 73:2424–2428.

Hamill OP, Marty A, Neher E, Sakmann B, Sigworth FJ (1981) Improved patch-clamp techniques for high-resolution current recordings from cells and cell-free membrane patches. Pfluegers Arch 391:85–100.

Hille B (1992a) Structure of channel proteins. In: Ionic channels of excitable membranes, 2d ed, pp 236–258. Sunderland, MA: Sinauer.

Hille B (1992b) Evolution and diversity. In: Ionic channels of excitable membranes, 2d ed, pp 525–544. Sunderland, MA: Sinauer.

Hille B (1992c) G Protein-coupled mechanisms and nervous signaling. Neuron 9:187–195.

Honore H, Martin C, Mironneau C, Mironneau J (1989) An ATP-sensitive conductance in cultured smooth muscle cells from pregnant rat myometrium. Am J Physiol 257:C294–C305.

Ifune CK, Steinbach JH (1991) Voltage-dependent block by magnesium of neuronal nicotinic acetylcholine receptor channels in rat phaeochromocytoma cells. J Physiol (Lond) 443:683–701.

Igusa Y (1988) Adenosine 5'-triphosphate activates acetylcholine receptor channels in cultured *Xenopus* myotomal muscle cells. J Physiol (Lond) 405:169–185.

Inoue K, Kenimer JG (1988) Muscarinic stimulation of calcium influx and norepinephrine release in PC12 cells. J Biol Chem 263:8157–8161.

Inoue K, Nakazawa K (1992) ATP receptor-operated Ca^{2+} influx and catecholamine release from neuronal cells. News Physiol Sci 7:56–59.

Kolb HA, Wakelam MJO (1983) Transmitter-like action of ATP on patched membrane of myoblasts and myotubules. Nature 303:621–623.

Krishtal OA, Marchenko SM, Obkuhov AG (1988) Cationic channels activated by extracellular ATP in rat sensory neurons. Neuroscience 27:995–1000.

Lu Z, Smith DO (1991) Adenosine 5'-triphosphate increases acetylcholine channel opening frequency in rat skeletal muscle. J Physiol (Lond) 436:45–56.

Majid MA, Okajima F, Kondo Y (1992) Characterization of ATP-receptor which mediates norepinephrine release in PC12 cells. Biochim Biophys Acta 1136:283–289.

Marty A, Neild TO, Ascher P (1976) Voltage sensitivity of acetylcholine currents in *Aplysia* neurons in the presence of curare. Nature 261:501–503.

Mathie A, Cull-Candy SG, Colquhoun D (1987) Single-channel and whole-cell currents evoked by acetylcholine in dissociated sympathetic neurons of the rat. Proc R Soc Lond [Biol] 232:239–248.

Nakazawa K, Hess P (1993) Block by calcium of ATP-activated channels in pheochromocytoma cells. J Gen Physiol 101:377–392.

Nakazawa K, Matsuki N (1987) Adenosine triphosphate-activated inward current in isolated smooth muscle cells from rat vas deferens. Pfluegers Arch 409:644–646.

Nakazawa K, Fujimori K, Takanaka A, Inoue K (1990a) Reversible and selective antagonism by suramin of ATP-activated inward current in PC12 phaeochromocytoma cells. Br J Pharmacol 101:224–226.

Nakazawa K, Fujimori K, Takanaka A, Inoue K (1990b) An ATP-activated conductance in pheochromocytoma cells and its suppression by extracellular calcium. J Physiol (Lond) 428:257–272.

Nakazawa K, Inoue K, Fujimori K, Takanaka A (1990c) ATP-activated single-channel currents recorded from cell-free patches of pheochromocytoma PC12 cells. Neurosci Lett 119:5–8.

Nakazawa K, Fujimori K, Takanaka A, Inoue K (1991a) Comparison of adenosine triphosphate- and nicotine-activated inward currents in rat phaeochromocytoma cells. J Physiol (Lond) 434:647–660.

Nakazawa K, Inoue K, Fujimori K, Takanaka A (1991b) Effects of ATP antagonists on purinoceptor-operated inward currents in rat phaeochromocytoma cells. Pfluegers Arch 418:214–219.

Neuhaus R, Reber BFX, Reuter H (1991) Regulation of bradykinin-and ATP-activated Ca^{2+}-permeable channels in rat pheochromocytoma (PC12) cells. J Neurosci 11:3984–3990.

Peters JA, Malone HM, Lambert JJ (1992) Recent advances in the electrophysiological characterization of 5-HT_3 receptors. Trend Pharmacol Sci 13:391–397.

Suzuki H (1985) Electrical responses of smooth muscle cells of the rabbit ear artery to adenosine triphosphate. J Physiol (Lond) 359:401–415.

Ueno S, Harata N, Inoue K, Akaike N (1992) ATP-gated current in dissociated rat nucleus solitarii neurons. J Neurophysiol 68:778–785.

Vernino S, Amador M, Luetje CW, Patrick J, Dani JA (1992) Calcium modulation and high calcium permeability of neuronal nicotinic acetylcholine receptors. Neuron 8:127–134.

Yellen G (1982) Single Ca^{2+}-activated nonselective cation channels in neuroblastoma. Nature 296:357–359.